Venus nightside ionospheric holes

Walter R. Hoegy[1] and Joseph M. Grebowsky[2]

Received 14 May 2010; revised 26 August 2010; accepted 4 October 2010; published 18 December 2010.

[1] Pioneer Venus Orbiter (PVO) measured the ionosphere and atmosphere of Venus for 13 years 10 months yielding a rich data set of archived data from a complement of instruments. One particularly striking feature seen was the occurrence of deep localized nightside ionization depletions commonly called holes. A number of theories have been put forth to explain their observed characteristics, but there is still no consensus on their source. A possibly related phenomenon in the Venus nightside ionosphere is the occurrence of "disappearing" or severely disturbed ionospheres characterized by deep, widespread plasma depletions in almost the entire nightside. This paper reexamines the holes and "disappearing ionospheres" and other characteristics of the nightside ionosphere during solar maximum using a more extensive database than earlier studies. The hole locations, occurrences, and dependencies on solar wind dynamic pressure (Psw) are analyzed, and a comparison is made with earlier studies. It is shown that there is no Psw threshold for holes to occur and at Psw values greater than ~9 nPa, hole occurrence decreases while the occurrence of severely disturbed orbits increases, suggesting that holes may evolve into severely disturbed orbits. Other characteristics of the nightside are shown to be influenced by solar wind pressure to varying degrees; for example, the density integrated along the orbit path below the ionopause, and the median density at low altitudes exhibit strong inverse correlation with Psw, while the peak density is nearly independent of Psw.

Citation: Hoegy, W. R., and J. M. Grebowsky (2010), Venus nightside ionospheric holes, *J. Geophys. Res.*, *115*, A12322, doi:10.1029/2010JA015675.

1. Introduction

[2] The low-altitude nightside ionosphere was sampled during the first 3 years of the Pioneer Venus Orbiter (PVO) mission when periapsis was kept nearly constant at about 150 km. This period during the active part of the solar cycle was typically characterized by an extended Venus dayside ionosphere that was the source of a copious nightside ionosphere via transport of ionization across the terminator [*Kliore et al.*, 1991]. The nightside orbits 19–130, 243–354, and 467–578 were used to study the nightside ionospheric morphology and its responses to changes in the solar wind dynamic pressure. There are three unique nightside ionosphere states: (1) a "normal" ionosphere with density continuously increasing with decreasing altitude above the ionospheric peak; (2) an ionosphere with deep localized depressions in the plasma density called "holes"; and (3) an irregular, low-density, severely disturbed ionosphere called a "disappearing" ionosphere. The characteristics and dependence of these states on solar wind dynamic pressure (Psw) at the bow shock or the magnetic pressure (Pb) at the ionopause are analyzed using the GSFC Unified Abstract Data System (UADS). UADS contains 12 s averages of data from most of the PVO instruments and is available from the authors.

1.1. Data Sets and Orbit Characteristics: Normal, Holes, and Severely Disturbed

[3] The analysis uses ion densities from two of the plasma instruments on PVO: (1) the Orbiter Electron Temperature Probe (OETP) UADS total ion density Ni and the high-resolution density (HIRES Ni) from the Planetary Data System (PDS); and (2) the Orbiter Ion Mass Spectrometer (OIMS) UADS O^+, and UADS total ion density (ITOT). Also used as a baseline for comparison is the empirical model of average ionosphere density of *Theis et al.* [1984], derived from the PVO OETP density measurements; the model is a function of solar zenith angle (SZA) and altitude. The solar wind pressure was obtained from the Goddard Space flight Center Space Physics Data Facility (http://cohoweb.gsfc.nasa.gov/cw.html).

[4] As an introduction to the data used in this study and to exhibit the different states of the nightside ionosphere, Figure 1a illustrates orbit 547 an example of a "normal" periapsis pass through the nightside, Figure 1b illustrates orbit 537 having two clearly defined holes, Figure 1c illustrates orbit 490 an example of a "disappearing" or severely disturbed ionosphere, and Figure 1d illustrates orbit 95 illustrating the frequent occurrence of a mixture of conditions, i.e., irregularities on the inbound leg and a hole on the

[1]Leelanau Research, Empire, Michigan, USA.
[2]NASA Goddard Space Flight Center, Greenbelt, Maryland, USA.

Copyright 2010 by the American Geophysical Union.
0148-0227/10/2010JA015675

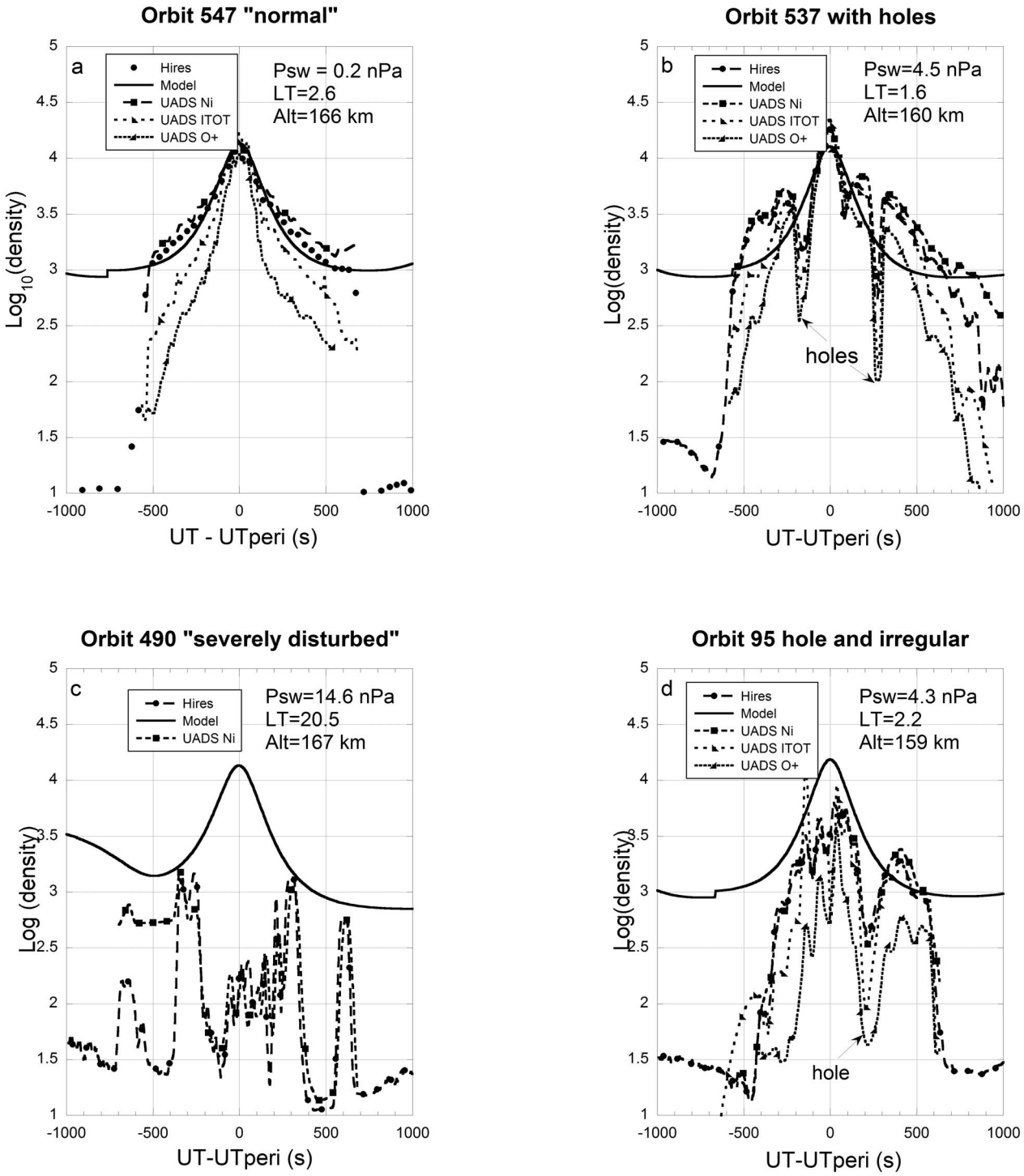

Figure 1. Various states of the nightside ionosphere: (a) orbit 547 normal, (b) orbit 537 with holes, (c) orbit 490 severely disturbed, and (d) orbit 95 with irregularities inbound and a hole outbound. LT denotes local time and ALT denotes the altitude in km.

outbound leg. The orbits in Figure 1 are "best" examples of the states; many nightside passes appear as mixtures of these states or poorly defined states with, e.g., multiple holes on one side of periapsis, or shallow holes.

[5] Orbit 547 depicts a filled up undisturbed ionosphere, the "normal" state at the peak of the solar cycle; the OETP HIRES and UADS Ni densities agree closely with the model average density. The sharp density gradients at high-altitude exhibited by HIRES Ni mark the ionopause positions (taken as the 10^2 cm^{-3} point). The greater time resolution of the HIRES data makes it especially useful for more precisely locating sharp features such as the ionopause position.

Differences between the OETP density (HIRES and UADS Ni) and the OIMS total density (ITOT) is useful for determining the likely locations of high ion drift since plasma drift modifies the assumed (i.e., spacecraft ram direction) entry angle of ions into the orifice of the ion mass spectrometer. The OETP ion density is insensitive to ion drift due to the cylindrical geometry of the Langmuir probe. At low altitudes the comparison of the O^+ density with Ni or ITOT, provides a location where molecular ions become significant. Orbit 537 illustrates an orbit with clearly defined holes displayed by all four experimental densities. An interesting feature is that the densities outside the holes rise above the model average, a characteristic seen with clearly defined holes. Orbit 490 illustrates the severely disturbed state, or the disappearing ionosphere [*Cravens et al.*, 1982]. No OIMS data were available for this highly disturbed orbit. Orbit 95 illustrates a mixture of irregularities (on the inbound leg) and the occurrence of a hole on the outbound leg. The irregularities also appear on the outbound edge of the hole, particularly in the O^+ density, which is minor compared to H^+ as seen by the difference between the O^+ density and the total ion density, ITOT. Irregularities occur frequently and could be part of the hole evolution or interaction with plasma outside with the hole. The irregularities are not examined in this paper.

[6] The Psw values for the four-sample orbits in Figure 1 imply that the solar wind pressure (Psw) is an important influence on the states of the Venus nightside ionosphere that change from full-up to depleted ionospheres with increasing pressure. However, these orbits were chosen as "best examples" and do not prove this relationship. A statistical examination of hole and severely disturbed orbit occurrence with Psw is given in section 3.

1.2. Previous Studies of Holes and Disappearing Ionospheres

[7] *Brace et al.* [1980] and *Taylor et al.* [1980] published the first papers on the discovery of Venus nightside ionospheric holes. A seminal paper by *Brace et al.* [1982], sketched the spatial and temporal distribution of the holes by analyzing the first 3 years of nightside passes with the OETP data, and most subsequent papers have used the same sequence of Venus orbits. *Brace and Kliore* [1991] summarized our knowledge of the Venus ionosphere, including the holes, up to the end of the PVO mission based on papers published up to that time. Other hole studies have been published since 1991, but the basic characteristics of the holes of *Brace et al.* [1982] are still commonly accepted. The holes are a common nightside feature near the maximum of the solar cycle, which appear as deep troughs in electron density (N_e) that extend several hundred kilometers along the orbit. The holes have typically locally enhanced magnetic fields parallel to the sun-planet line and dual electron temperatures, T_e. The magnetic fields tend to have opposite polarities when two holes are encountered on the same orbit on opposite sides of periapsis. The relative inward-outward sense of the magnetic field directions is directly related to the interplanetary magnetic field (IMF) direction, consistent with draping within the ionosphere [*Marubashi et al.*, 1985]. Since the day-to-night flow of plasma carries "frozen-in" magnetic field lines, the sharp density depletions in the holes would be expected to correspond to an increase in the B field, and typically there is total pressure balance (magnetic plus thermal plasma) inside and outside of the holes [*Brace et al.*, 1982].

1.3. Theories of Holes

[8] Several possible sources have been suggested for the origin of holes: outward loss of plasma by the interplanetary magnetic field lines pulling out of the ionosphere [*Brace et al.*, 1982]; magnetic field-aligned, auroral-like electric fields that eject plasma [*Grebowsky and Curtis*, 1981]; gravitational acceleration downward into the lower atmosphere chemical sink [*Grebowsky et al.*, 1983]; plasma channels cut by solar wind erosion of the magnetic polar regions [*Pérez-de-Tejada*, 2004]; and a deformation of the nightside ionopause toward the antisolar region at low magnetic latitudes by magnetosheath pressure [*Marubashi et al.*, 1985]. *Brace et al.* [1982] suggested the persistent occurrence of two holes with limited longitude extent to account for the observation of B reversals in hole pairs and to explain why some orbits appear to contain only one hole: the absent hole is not seen because the orbit passes through a different longitude (or local time) from that of the hole. The possible movement of holes is discussed in section 2. The plasma channel interpretation of holes by *Pérez-de-Tejada* [2004] has the same type of magnetic field topology but with the holes extending from the polar cap to low latitudes. The electric field and gravitational collapse models would possibly lead to two meridionally elongated holes with opposite field polarities separated by a dense plasma region in the midnight region. The reasoning for this scenario is that plasma losses occur downward along vertical, lower atmosphere-connecting draped magnetic field lines; this would be reasonable if "zonal" horizontal ion flow at low latitudes were primarily responsible. For the ionopause pinching mechanism of *Marubashi et al.* [1985], the holes would simply be PVO crossings from the ionosphere into the tailward draped field lines of the ionosheath and back into the ionosphere. This scenario also relies on the dominance of low-latitude magnetoplasma effects. A consensus has yet to be reached on which is the best explanation for the holes.

[9] The uncertainty in the hole origin also extends to MHD modeling. A comprehensive 3-D model that includes a two-component plasma, solar wind protons, and ionospheric O^+ with chemistry [*Tanaka and Murawski*, 1997] found only weak evidence for the production of a hole, with the possibility that there are four. They pointed out that four small depressions arranged around the antisolar point could perhaps be holes or perhaps the holes are dynamic phenomena.

2. Hole Characteristics and Location

[10] The orbits during the first 3 years examined by *Brace et al.* [1982] and subsequent papers, including this paper, are those with periapsis local times on the nightside of the terminator: the orbits 19–130, 240–354, and 471–581. There is an element of subjectivity in the identification of holes, a point emphasized by *Brace et al.* [1982]. This has been the case in subsequent studies including this paper. On orbit passes with smoothly varying electron densities on the outer ionosphere side of the ionopause crossings the identification of the abrupt depletion of a hole is "obvious," while on orbits crossing somewhat disturbed or irregular ionospheres

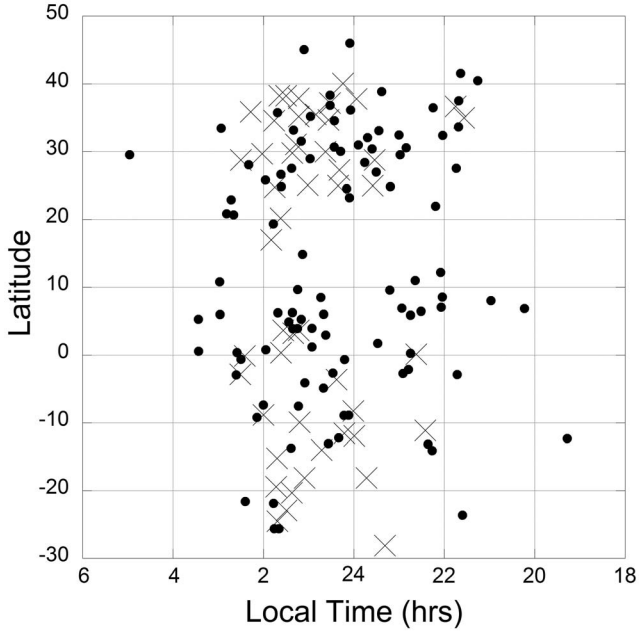

Figure 2. Latitude-local time domain of holes from the first three seasons of PVO data. The *Brace et al.* [1982] holes (denoted B holes) are large crosses. This paper's holes are dots.

it is often not clear if there is one, two or more, or no holes present. In the process of categorizing the holes, *Brace et al.* [1982] stated that some structures that were somewhat suggestive of a hole were not counted as such, and were not selected on orbits where there were several density depressions rather than single troughs on the inbound or outbound orbital legs. Thus using only "clean" cases by a visual inspection of plotted electron densities, *Brace et al.* [1982] identified about 50 holes during the first 3 years of nighttime passes.

[11] Some of the other studies of hole properties were made by *Marubashi et al.* [1985] and *Mahajan and Oyama* [2001]. Both used somewhat restricted observations compared to all data available in the archives. Using OIMS O^+ and O_2^+ density measurements and requiring a depth of a factor of 2 below the outside density and a trough width of more than one minute along the orbit, *Marubashi et al.* [1985] found 55 holes. However, they used only the first 2 years of PVO data and did not distinguish whether some holes had O_2^+ as major ion and thus could have been passing through a lower ionization layer peak and not a hole. Using the complete first 3 years of OIMS O^+ data, *Mahajan and Oyama* [2001] identified about 75 holes from a visual search through orbital plots. The sensitivity of the OIMS data to the presence of ion flows, and regions where O^+ was a minor species (i.e., H^+ or molecular ions were dominant) could have introduced some extraneous structures in the O^+ profiles. Also, there were data gaps in the OIMS archived ion composition measurements that were not present in OETP ion and electron density measurements. Hence, these studies did not employ the most complete measurements available to study the nightside ionosphere. The number of orbits in each of the first 3 years containing sufficient O^+ versus sufficient OETP Ni to search for holes is (1) first year, O^+ 77 orbits, OETP 96 orbits; (2) second year, O^+ and OETP 57 orbits; and (3) third year, O^+ 78 orbits, OETP 105 orbits. Conclusions reached from using incomplete data sets could lead to different results when the smaller data sets contain different properties such as hole occurrence, orbit coverage in latitude and longitude, or values of the solar wind pressure. Ignoring the third year of data could bias conclusions reached using a more limited data set.

[12] The present study selects holes using the OETP ion density measurements with the criteria that the density depression be at least a factor of 2, and that the hole width be greater than 30 s (300 km) along the orbit. The presence of a well-ordered magnetic field above the ionosphere was not a requirement for a hole to exist, as was the case of *Marubashi et al.* [1985]; holes are selected only on the basis of a density depression, once selected their magnetic field characteristics can be examined. Out of the 258 nightside periapsis orbits from the first three seasons ~103 holes were found, some multiple, thus 70 orbits out of 258 analyzed or 27% were found to have holes. The mean density depression from the top of the sides to the depth of the hole was found to be a factor of 9 and the mean duration along the orbit 143 s (~1430 km along orbit). The complete list of the holes is available from the authors. A quantitative selection criterion was not used for the severely disturbed cases, making this collection more subjective. The classification of orbits into three ionospheric states is used to develop occurrence statistics with respect to solar wind pressure.

[13] The location of the holes in latitude and local time is given next along with a comparison with the *Brace et al.* [1982] holes. The dawn/dusk bias of the holes singled out by *Brace et al.* [1982] is shown below to be mainly due to PVO data availability in the dawn and dusk sectors, although physical processes contribute to some of the bias. In a related study of dawn/dusk bias, *Phillips et al.* [1988, p. 3940] found that asymmetries in the ionopause height (dawn higher than dusk) was due to "flow aberration from planetary motion" and "solar wind dynamic pressure sampling bias" and stated that "No additional physical mechanisms are needed to generate this asymmetry."

[14] *Brace et al.* [1982, p. 201] found that holes are detected predominately in two regions; a northern zone of latitude 20°N–40°N, and a southern zone of latitude 0°–25°S; and qualified these zones as being "Somewhat arbitrarily defined owing to poor statistics." The local time range of the hole occurrence was found to be ~2330 to ~0230 LT, offset toward the dawn terminator by about 1 h. *Marubashi et al.* [1985] found a similar aliasing toward dawn and also showed that there was a dawn/dusk aliasing in available orbits during the first 2 years. This paper shows that this orbit bias persists when the third year of data is included. *Marubashi et al.* [1985] did have many higher latitude (and therefore higher altitude) events in their ensemble of holes, possibly because they used OIMS O^+ measurements that are affected by ion flows which are known to exist at high altitudes and also perhaps encountered plasma plumes above the ionopause. A comparison of the holes found in this paper (dots), with the *Brace et al.* [1982] holes (large cross, denoted B holes) are shown in Figure 2.

[15] Since there was no list in the work by *Brace et al.* [1982] giving the orbit numbers and UTs of their B holes,

the latitude/local time location of their Figure 4a holes were digitized. The error in digitizing the B holes is less than 1.4° latitude and 0.16 h local time (or 2% of the respective widths of their x and y scales). Only 29 of the 55 B holes could be matched by holes found in this study, and many of our holes had no matching B hole. A careful examination of the PVO data was unable to find any holes near the unmatched B holes within an error tolerance of 5%; this could be due to a plotting in error in *Brace et al.*'s [1982] Figure 4a. The hole locations correspond to the deepest density point in latitude and local time. Displaying the start-to-end points of the holes along PVO's polar orbit would widen their latitude extent but not significantly widen their local time coverage, thus the disparity between the B holes and the holes found in this study remains.

[16] The aliasing toward the dawn sector shown first by *Brace et al.* [1982] and later by *Marubashi et al.* [1985] is mainly due to the asymmetry in data availability in the dawn versus the dusk sectors. Although the basic PVO orbit traverses through all local times uniformly premidnight and postmidnight, data are not uniformly available due to vagaries of spacecraft operations turning on instruments. *Marubashi et al.* [1985] used O^+ data exclusively for the first 2 years to search for holes and found a ratio of dawn/dusk orbits of ~3; however, many orbits that contain OETP densities lack O^+ data which affects the number of orbits available to search for holes; and they omitted all orbits available during the third year. Employing the first three seasons and using OETP data or all OIMS data, the dawn/dusk ratio of available data is ~1.4. The dawn/dusk ratio of holes found in this study is ~1.6, giving a physical or true bias in the formation of holes dawn/dusk of 1.14 ± 0.1. Thus orbital coverage is a strong influence shifting the apparent hole occurrence toward dawn, however, there are physical causes such as the asymmetry in ion flow first demonstrated by *Miller and Whitten* [1991], and solar aberration could contribute to the bias as suggested by *Brace et al.* [1982] and demonstrated by *Phillips et al.* [1988] to make a small contribution to asymmetry in ionopause height. In addition, asymmetric pickup of exospheric ions by magnetosheath electric and magnetic fields was shown to affect ionopause height [*Phillips et al.*, 1988]. Another physical process that could influence asymmetries in hole occurrence and ionopause height is the Magnus force [*Pérez-de-Tejada*, 2006].

[17] The low-latitude gap in the hole occurrences and the offset of the gap northward of the equator is due to the orbit configuration, namely the location of periapsis, which (during the first 3 years) varies from 18.5° to 15.1° north, and the weakening of the mechanism producing holes at altitudes below 200 km. *Grebowsky and Curtis* [1981, p. 1273] noted that "holes are typically not detected below 200 km" [see also *Brace et al.*, 1980]; and we find no holes below 167 km. One would expect ion-neutral collisions to relax the coupling to the magnetic field at low altitudes. As a result, the magnetic field which obviously plays a role in hole development at high altitudes cannot play a similar role at the lower PVO altitudes.

[18] *Brace et al.* [1982] suggested that holes are always present and that they are not seen on every orbit, nor always found on consecutive orbits because they have a limited extent in latitude and local time and change position faster than the ~24 h period of the slow spatially varying PVO orbit tracks from orbit to orbit. *Pérez-de-Tejada* [2004] noted that the location of holes should depend on IMF orientation; this presents a mechanism for holes to move away from the orbit path as the IMF orientation changes from orbit to orbit. Let us compare the movement of the detected holes with that of the periapsis position in latitude and local time or longitude. The average periapsis movement for consecutive orbits (24 h period) during the first 3 years is −0.0135° latitude and 0.107 h local time (1.6° longitude). The median offset of holes relative to periapsis position is 14° in latitude and 4.7° in longitude, corresponding to a median time difference from periapsis of 162 s. The median transit time through holes is 133 s, and the typical UT window for observing an inbound or an outbound hole is approximately 500 s. The inbound holes are located within a swath of about 25° in latitude from periapsis, which itself varies by only 3.3° in latitude over the first 3 years of data; thus, the latitude position of periapsis on all orbits does not influence observing a hole. This means that holes cannot escape detection by moving in latitude due to the north to south sweep of consecutive orbits. In contrast, holes are seen within a swath of only about 0.67 h in local time from periapsis, which itself changes by 0800 LT time during the 3 year measurement period, thus holes can easily escape detection by moving by about 1 h or more in local time. Holes are observed only when they happen to be within about 0.93 h of periapsis. For inbound holes, the observed occurrence is the ratio of number of holes to the number of orbits in each of the 3 years: 16/96 = 0.167, 13/57 = 0.22, and 17/105 = 0.16, respectively. Compare these occurrences with the chance of finding holes in each of the 3 years when they are within 0.96 h of periapsis for the periapsis ranges of 6, 3.5, and 7.5 h; the fractions are 0.16, 0.23, and 0.12, respectively. Hence the estimated probabilities of finding holes agree approximately with the occurrence of holes in each of the 3 years. This result supports the *Brace et al.* [1982] supposition that holes almost always exist. Section 3.1 demonstrates that at high Psw values, holes either do not exist or cannot be detected when the nightside is severely depleted. It is noted that on many periapsis passes there are hints of a hole (shallow holes that were not counted) which could be due to the orbit skimming the edge of the hole.

3. Dependence of the Nightside Ionosphere on Variations in Psw

[19] This section explores the influence of solar wind dynamic pressure on the three states of the nightside ionosphere by determining the occurrence of holes and severely disturbed orbits. The dependence of the density maximum, median low-altitude density and density content along the orbit track within the ionosphere on Psw is examined and it is found that the orbital path integral and averaged density are better correlated with Psw than the maximum density; this is due to dynamical processes having a strong influence on structure, while Psw controls net density content. Finally, dependence on Psw of some of the hole characteristics is discussed. This study does not treat in any detail the influence of the magnetic field on holes, except to note a few observations on the orientation and smoothness of the field in holes.

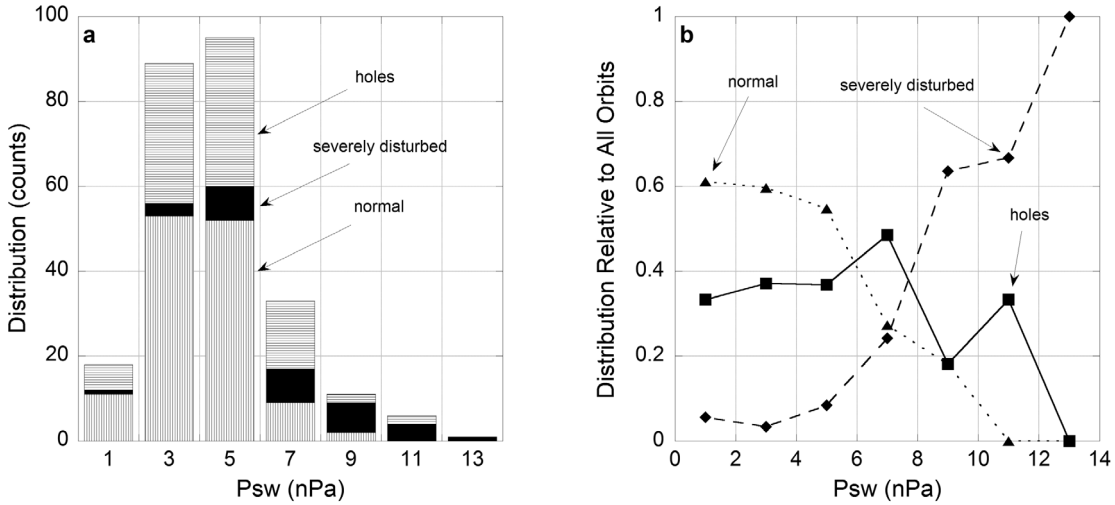

Figure 3. (a) Psw distributions in number of orbits for the different categories of orbits: with holes, severely disturbed, and normal ionospheres. (b) Ratio of hole, severely disturbed, and normal orbits to the distribution for all orbits during the first 3 years.

3.1. Hole and Severely Disturbed Occurrence Versus Psw

[20] In this section the dependence of the hole and disappearing ionosphere occurrences on Psw is explored. It is shown that there appears to be no lower Psw threshold for the occurrence of holes. This supports the *Brace et al.* [1982] contention that holes always exist, and it was shown in section 2 that the chance of observing holes (if they move randomly in local time) is very close to the occurrence frequency of holes. Further, the theories of scavenging by *Pérez-de-Tejada* [2004] and erosion by *Brace et al.* [1982] would imply that the strength and direction of the solar wind encountered during the low periapsis lifetime of PVO was always conducive to hole formation. In contrast, there appears to be a Psw threshold for the formation of disappearing nightside ionospheres. Thus, at very high solar wind pressure, the holes either expand their latitude extent becoming severely depleted regions, or the surrounding plasma is eroded and the mechanism generating the holes diminishes. Thus the disappearing ionospheres may be formed by a throttling off of the supply of ionization outside of the holes until the nightside plasma pressure becomes small compared to the magnetic pressure and no longer supports the localized buildup of magnetic pressure associated with the holes.

[21] Figure 3 depicts the solar wind dynamic pressure distribution for the different nightside ionization states: orbits with holes, severely disturbed orbits, and normal orbits. The distributions for each category are plotted as the number of orbits in the Psw bins of width 2 nPa in Figure 3a. The Psw distribution function for all orbits (Figure 3a) has a median of 4.5 nPa and a tail slightly higher than a Gaussian or Poisson fit would exhibit. The ratio of the three distributions to the total distribution clearly displays in Figure 3b the relative distribution of the three states in each of the solar wind pressure bins. For Psw less than 4 nPa about 60% of orbits are normal, ~35% have holes and less than 10% are severely disturbed. It appears that there is no solar wind pressure threshold for the occurrence of holes, but that they exhibit a decreasing occurrence trend at values of Psw greater than 7 nPa. The occurrence of severely disturbed orbits increases above a Psw value of ~6 nPa, and the normal orbits decrease above ~5 nPa. The uncertainties in the relative fractions increase above 7 nPa due to the low total number of orbits at these high Psw values, but the trends shown in Figure 3b are significant. At high Psw when the nightside is severely disturbed, the holes are no longer readily identified, or are no longer generated as mentioned above. *Mahajan and Oyama* [2001, p. 1866] concluded "that a hole will generally be seen when Psw is moderate (2.5 to 4.5 nPa) and a disappearing ionosphere will be seen when Psw is high." Figure 3b shows that the occurrence of holes versus Psw is approximately constant until they are replaced by severely disturbed orbits for Psw above ~7 nPa.

3.2. Density and Ionopause Variation With Psw

[22] The dependence of other indicators of ionization content and its dependency on the solar wind pressure is examined next. *Brace et al.* [1980] showed that ionopause altitude, Ip, on the dayside varies inversely with the magnetic field pressure, Pb, measured just outside the ionopause. They also showed the close linear relationship between Pb and the solar wind pressure, Psw multiplied by $\cos^2$(SZA) just outside the bow shock. The height of the terminator ionopause would also be expected to be controlled by the solar wind pressure at the bow shock or the magnetic pressure at the ionopause, and it follows that total ionization and other characteristics of the nightside which is dependent on terminator Ip would also exhibit a dependency on Psw or Pb. Figure 4 shows the inverse relation of the terminator ionopause with Pb, in analogy with the *Brace et al.* [1980] dayside relationship.

[23] Following the example of *Brace et al.* [1980], the fit in Figure 4 has the form altitude = A + B exp(C Pb) with the coefficients A = 558, B = 1062, and C = −2.45. *Phillips et al.* [1985] demonstrated the nearly linear relationship between Ip altitude and the natural logarithm of the magnetic

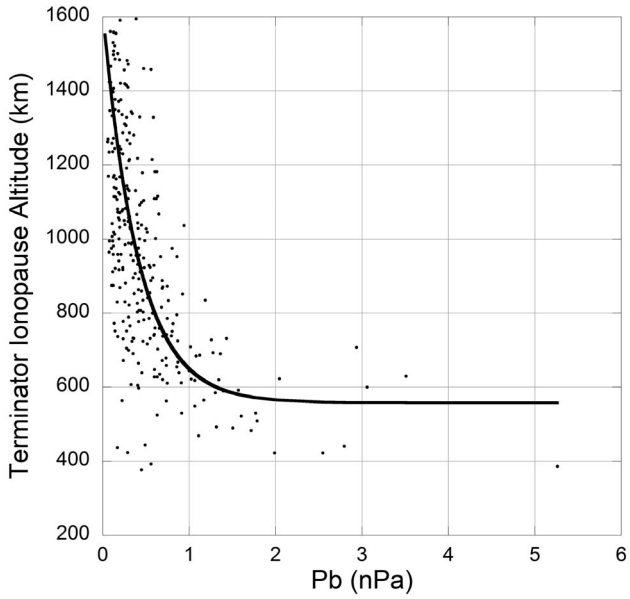

Figure 4. Plot of terminator ionopause altitude versus the magnetic pressure just outside the ionopause. The terminator ionopause data are taken in a 2 h interval about 0600 and 1800 LT from inbound and outbound ionopause crossings.

pressure, obtaining different coefficients using a broad SZA range from 0° to about 120°.

[24] A number of other studies have shown the solar wind pressure control of the nightside density. *Miller and Knudsen* [1987] examined cross-terminator flows which are modified by solar wind pressure and changes in ionopause height. They compared a normalized ionopause height to the median of the ratio of Ni divided by the *Theis et al.* [1980, 1984] density model over the altitude range 170–200 km using ion densities from the Pioneer Venus Orbiter Retarding Potential Analyzer (ORPA). They showed that the median nightside ORPA ion density in the altitude range 170–200 km exhibited an increasing trend with ionopause height. Using OETP Hires Ni data, Figure 5 compares the normalized median Ni for the same 170–200 km altitude region versus ionopause height in Figure 5a and versus solar wind pressure in Figure 5b. To compare different measures of density, Figure 6a shows the variation of the integrated normalized density and Figure 6b the maximum normalized density versus solar wind pressure. The density is normalized by dividing by the *Theis et al.* [1984] density model. The nightside density is seen to be affected by the solar wind pressure, but it is also subjected to a variety of dynamical processes that can produce localized perturbations in the nightside through the magnetic field orientation, the direction of ion flow, and the location of precipitating electrons resulting in large scatter seen in the plots in Figures 5 and 6.

[25] The plots in Figure 5 use the ratio of Ni to the *Theis et al.* [1984] model in the nightside; use of the ratio reduces the solar zenith angle and altitude dependence of the density to enhance the dependence on Ip and Psw. However, unlike *Miller and Knudsen* [1987], use is not made of a normalized ionopause height so that the correlation is made directly to the controlling variables, i.e., Ip and Psw. Use of the density normalization does help to reduce the solar zenith angle dependence. The correlation coefficient of the normalized median density with Ip, Psw, and SZA is 0.43, −0.44, and 0.0, respectively. The correlation coefficients of the unnormalized median density with Ip, Psw, and SZA is 0.34, −0.41, and 0.54, respectively, exhibiting the strong solar zenith angle dependence of the density. The large amount of scatter is due to the dynamics of the nightside and neglect of other variables controlling flow of ionization, in addition to other sources and sinks. The result of Miller and Knudsen that ionopause height has control over the nightside density is supported by the OETP data shown in Figure 5. A simultaneous fit to Ip, SZA, and Psw yields a better fit than a linear fit made to only one of the variables.

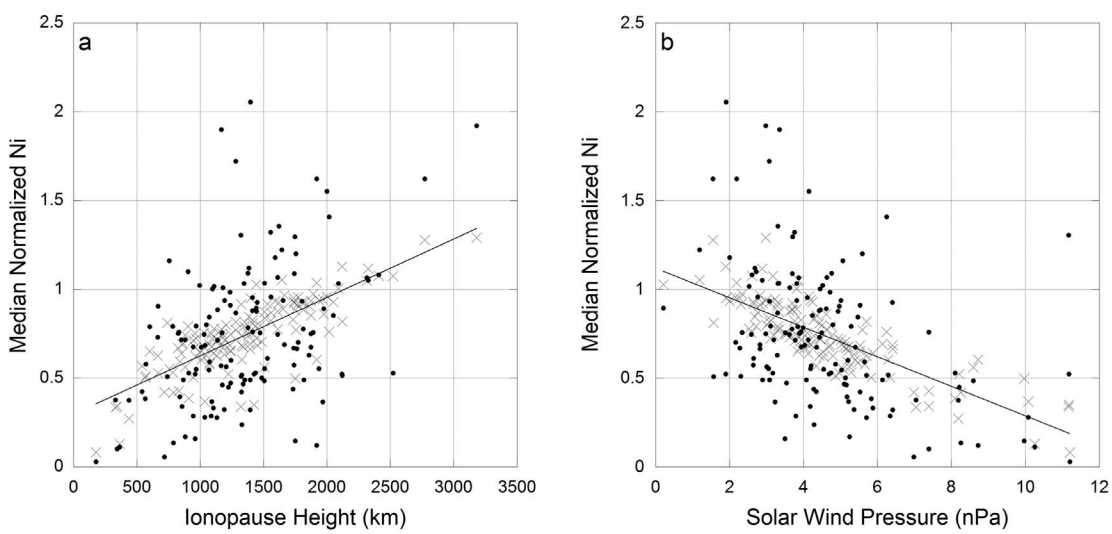

Figure 5. (a) Normalized median Ni over the altitude range 170–200 km plotted versus ionopause height. Dots are the data points, the line with crosses is a simultaneous linear fit to Ip, Psw, and cos(SZA). The straight line is a linear fit to the data. (b) The same data and fits are plotted versus Psw.

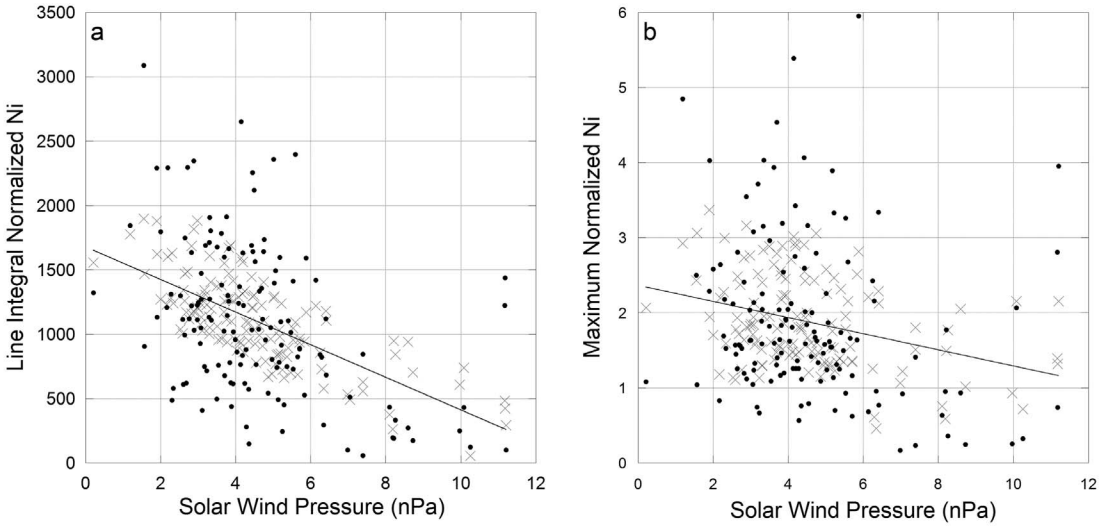

Figure 6. (a) Line integral of normalized OETP Ni versus Psw. (b) Maximum Ni normalized by *Theis et al.* [1984] model versus Psw. The symbols have the same meaning as Figure 5.

[26] *Zhang et al.* [1990] and *Kliore et al.* [1991] used vertical electron content in addition to the nightside peak densities from Venus radio occultation measurements to explore their relationship with solar wind pressure. *Mahajan and Oyama* [2001] followed with a comparison of PVO maximum nightside O^+ densities from OIMS with Psw. Although they did not compute the correlation, their plot demonstrated an overall inverse relationship with Psw. Figure 6 shows the fits of the path integral of the OETP density and of the maximum density both normalized by the *Theis et al.* [1984] model. The path integral is the integral of the normalized density over the portion of the PVO orbital path through the ionosphere (at altitudes below the ionopause), and is analogous to the *Kliore et al.* [1991] vertical electron content.

[27] The path integral of the normalized density exhibits significant inverse correlation with solar wind pressure and correlation with ionopause height, Ip. The correlation coefficients with Psw, Ip, SZA, and altitude of the peak Ni are −0.44, 0.35, −0.25, and −0.2, respectively. For the unnormalized density path integral the coefficients are −0.42, 0.35, 0.4, and −0.3, respectively. Thus the correlation with Psw and Ip is unchanged by the density normalization. The results for the maximum Ni normalized by the *Theis et al.* [1984] model (see Figure 6b) show only a small dependency on solar wind pressure; the correlation coefficients with Psw, Ip, SZA, and altitude are −0.2, 0.1, −0.4, and −0.4, respectively. Analysis of the maximum unnormalized Ni yields the correlations for the same variables, −0.2, 0.1, 0.1, and −0.6, respectively. Thus the correlation of maximum Ni with Psw and Ip is again unchanged by normalization, and the normalization greatly changes the correlations with solar zenith angle and with the altitude of the maximum density. Thus the peak density of the nightside passes has a different solar zenith angle and altitude dependence than the *Theis et al.* [1984] density model. The peak density has a negligible dependence on solar zenith angle; a very different behavior from the *Theis et al.* [1984] model. Thus the solar zenith angle dependence of the *Theis et al.* [1984] Ni model well represents the densities in the 170–200 km region of Figure 5, but poorly represents the peak density and the integrated density. Examination of all the nightside orbits shows that the peak density exhibits great variations that are not represented by the model and that the model also becomes very poor in a region about 200 km below the ionopause. These effects are again due to the dynamic variability of the nightside, which is difficult to model.

[28] One of the results of *Kliore et al.* [1991] was that the negative slope of the integrated density variation with solar wind pressure at pressures below 6 nPa was less than the slope at pressures above 6 nPa. They attributed this change in slope to the addition of ionization from precipitating electrons at the higher pressures which begins to overwhelm the ionopause choking of the transterminator flow at all pressures. This may be happening, and a by-eye fit to Figure 6a tends to show this change in slope, however, the error bars are large enough to question whether this is statistically significant. There are an insufficient number of data points as seen in Figure 6a for this study to quantify the significance of the different slopes.

3.3. Hole Characteristics Versus Psw

[29] It was shown that many of the characteristics of the nightside ionosphere are controlled by the solar wind pressure, it is also of interest to examine whether hole characteristics such as altitude, density, depth, or width depend on Psw. *Mahajan and Oyama* [2001] concluded that since the solar wind pressure is a major factor controlling the nightside ionosphere, that it also controls the density and depth of the holes. This study finds that not all characteristics of the holes are controlled by solar wind pressure. The correlation coefficient of Psw with hole altitude, density, depth, and width is found to be 0.04, −0.18, 0.12, and 0.38, respectively. The altitude of the hole is defined as the altitude at the minimum density location, and the extent of the scatter in the data indicates no correlation with Psw. The hole minimum density shows a tendency to decrease with increasing Psw, however, the scatter precludes a firm conclusion of a

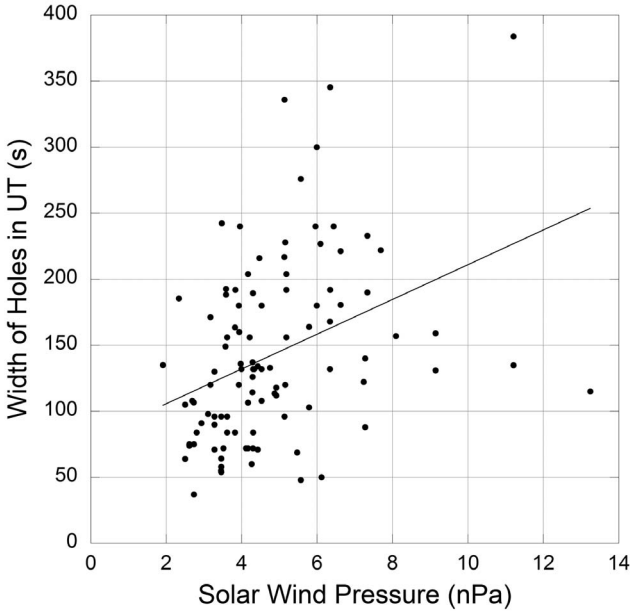

Figure 7. UT extent of the holes has a significant correlation with the solar wind pressure.

correlation. The hole depth is the altitude difference between the minimum density point and the altitude of the midpoint between the edges; there is no correlation of depth with Psw. Only the width, defined as the UT extent of the hole and shown in Figure 7, is significantly correlated with solar wind pressure. The reason may be due to the general depletion of the nightside ionosphere (shown in Figure 6) beginning the process of hole erosion and the transition to the severely disturbed state as described previously. As solar wind pressure increases, the outer boundary of the holes moves away from periapsis toward the terminator while the inner boundary moves closer to periapsis widening the hole. Analysis of the effect of solar wind pressure on location of the hole minimum point in local time, or latitude shows a null correlation (correlation coefficients of −0.05 and 0.1, respectively).

4. Summary

[30] Nightside Pioneer Venus Orbiter passes from the first 3 years were used to categorize orbits into three states: normal, containing holes or being severely disturbed. Analysis of the solar wind pressure (Psw) distribution of the states found that normal orbits occur mainly for values of Psw less than the mean at 5.4 nPa; the orbits with holes occur almost uniformly for values of Psw less than 12 nPa and that the severely disturbed orbits occur mainly at Psw greater than 8 nPa. There is no low Psw threshold for holes to occur, but a high threshold where they cease occurring and severely disturbed ionospheres dominate. The speculation of *Brace et al.* [1982] that holes are always present is supported by the finding that the fraction (chance) that holes are within local time range of a given orbit matches the fraction (occurrence) of observed holes. At Psw values greater than ~8 nPa, holes are swamped by the severely disturbed or "disappearing" ionospheres. The orientation of the magnetic field in the holes was not a criterion for a hole to exist; it was found that the most clearly delineated holes have steady fields aligned nearly parallel or antiparallel with the sun-Venus line but that for many holes, the fields are rapidly changing in direction and strength. An interesting corollary is that irregularly structured magnetic fields often occur when the density is smooth as for the "normal" orbits. Other aspects of the nightside ionosphere were examined for any dependence on Psw strength. The explicit (inverse) relationship of the terminator ionopause height with the magnetic pressure was given. It was found that the maximum density is poorly correlated with solar wind pressure (a correlation coefficient of −0.2), while the integrated density and the median density in the low-altitude interval 170–200 km both exhibit a strong inverse correlation of −0.44. The nightside ionosphere is a very dynamic region, and this is the source of much scatter in ionosphere density and other parameters leading to correlations less than 1/2. The holes are complex structures that are not yet completely understood with a number of theories that await future testing.

[31] **Acknowledgments.** The authors would like to thank the referees for helpful comments. This study was supported by grant NNX09AH51G from NASA GSFC.

[32] Philippa Browning thanks Hector Pérez-de-Tejada and Kushal Mahajan for their assistance in evaluating this paper.

References

Brace, L. H., and A. J. Kliore (1991), The structure of the Venus ionosphere, *Space Sci. Rev.*, *55*, 81–163, doi:10.1007/BF00177136.

Brace, L. H., R. F. Theis, W. R. Hoegy, J. H. Wolfe, J. D. Mihalov, C. T. Russell, R. C. Elphic, and A. F. Nagy (1980), The dynamic behavior of the Venus ionosphere in response to solar wind interactions, *J. Geophys. Res.*, *85*, 7663–7678, doi:10.1029/JA085iA13p07663.

Brace, L. H., R. F. Theis, H. G. Mayr, S. A. Curtis, and J. G. Luhmann (1982), Holes in the nightside ionosphere of Venus, *J. Geophys. Res.*, *87*, 199–211, doi:10.1029/JA087iA01p00199.

Cravens, T. E., et al. (1982), Disappearing ionospheres on the nightside of Venus, *Icarus*, *51*, 271–282, doi:10.1016/0019-1035(82)90083-5.

Grebowsky, J. M., and S. A. Curtis (1981), Venus nightside ionospheric holes: The signatures of parallel electric field acceleration regions?, *Geophys. Res. Lett.*, *8*, 1273–1276, doi:10.1029/GL008i012p01273.

Grebowsky, J. M., H. G. Mayr, S. A. Curtis, and H. A. Taylor Jr. (1983), Venus' nighttime horizontal plasma flow, 'magnetic congestion', and ionospheric hole production, *J. Geophys. Res.*, *88*, 3005–3012, doi:10.1029/JA088iA04p03005.

Kliore, A. J., J. G. Luhmann, and M. H. G. Zhang (1991), The effect of the solar cycle on the maintenance of the nightside ionosphere of Venus, *J. Geophys. Res.*, *96*, 11,065–11,071, doi:10.1029/91JA00672.

Mahajan, K. K., and K.-I. Oyama (2001), The central nightside Venus ionosphere: Dependence of ion concentration and plasma holes location on solar wind dynamic pressure, *Adv. Space Res.*, *27*(11), 1863–1868, doi:10.1016/S0273-1177(01)00320-9.

Marubashi, K., J. M. Grebowsky, H. A. Taylor Jr., J. G. Luhmann, C. T. Russell, and A. Barnes (1985), Magnetic field in the wake of Venus and the formation of ionospheric holes, *J. Geophys. Res.*, *90*, 1385–1398, doi:10.1029/JA090iA02p01385.

Miller, K. L., and W. C. Knudsen (1987), Spatial and temporal variations of the ion velocity measured in the Venus ionosphere, *Adv. Space Res.*, *7*(12), 107–110, doi:10.1016/0273-1177(87)90207-9.

Miller, K. L., and R. C. Whitten (1991), Ion dynamics in the Venus ionosphere, *Space Sci. Rev.*, *55*, 165–199, doi:10.1007/BF00177137.

Pérez-de-Tejada, H. (2004), Plasma channels and electron density profiles near the midnight plane in the Venus nightside ionosphere, *J. Geophys. Res.*, *109*, A04106, doi:10.1029/2002JA009811.

Pérez-de-Tejada, H. (2006), Magnus force in the Venus ionosphere, *J. Geophys. Res.*, *111*, A11105, doi:10.1029/2005JA011554.

Phillips, J. L., J. G. Luhmann, and C. T. Russell (1985), Dependence of Venus ionopause altitude and ionospheric magnetic field on solar wind dynamic pressure, *Adv. Space Res.*, *5*(9), 173–176, doi:10.1016/0273-1177(85)90286-8.

Phillips, J. L., J. G. Luhmann, W. C. Knudsen, and L. H. Brace (1988), Asymmetries in the location of the Venus ionopause, *J. Geophys. Res.*, *93*, 3927–3941, doi:10.1029/JA093iA05p03927.

Tanaka, T., and K. Murawski (1997), Three-dimensional MHD simulation of the solar wind interaction with the ionosphere of Venus: Results of two-component reacting plasma simulation, *J. Geophys. Res.*, *102*, 19,805–19,821, doi:10.1029/97JA01474.

Taylor, H. A., H. C. Brinton, S. J. Bauer, R. E. Hartle, P. A. Cloutier, and R. E. Daniell (1980), Global observations of the composition and dynamics of the ionosphere of Venus: Implications for the solar wind interaction, *J. Geophys. Res.*, *85*, 7765–7777, doi:10.1029/JA085iA13p07765.

Theis, R. F., L. H. Brace, and H. G. Mayr (1980), Empirical models of the electron temperature and density in the Venus ionosphere, *J. Geophys. Res.*, *85*, 7787–7794, doi:10.1029/JA085iA13p07787.

Theis, R. F., L. H. Brace, R. C. Elphic, and H. G. Mayr (1984), New empirical models of the electron temperature and density in the Venus ionosphere with application to transterminator flow, *J. Geophys. Res.*, *89*, 1477–1488, doi:10.1029/JA089iA03p01477.

Zhang, M. H. G., J. G. Luhmann, and A. J. Kliore (1990), An observational study of the nightside ionospheres of Mars and Venus with radio occultation methods, *J. Geophys. Res.*, *95*, 17,095–17,102, doi:10.1029/JA095iA10p17095.

J. M. Grebowsky, NASA Goddard Space Flight Center, Code 695, Greenbelt, MD 20771, USA.

W. R. Hoegy, Leelanau Research, 13601 S. Beaver Pond, Empire, MI 49630, USA. (wrhoegy@gmail.com)